

Submicrometer diameter micropillar cavities with high quality factor and ultrasmall mode volume

Yinan Zhang* and Marko Lončar

School of Engineering and Applied Sciences, Harvard University, 33 Oxford Street, Cambridge, Massachusetts 02138, USA

*Corresponding author: yinan@seas.harvard.edu

Received December 17, 2008; revised February 8, 2009; accepted February 9, 2009; posted February 13, 2009 (Doc. ID 105451); published March 17, 2009

We theoretically demonstrate high quality factor ($Q \sim 3 \times 10^6$) micropillar cavities with a record low mode volume [$V \sim 0.1(\lambda/n)^3$] based on the $\text{TiO}_2/\text{SiO}_2$ material system. The proposed cavities have Q/V that is 3 orders of magnitude larger than previously reported ones. We show that our cavity embedded with a diamond nanocrystal provides a feasible platform for cavity quantum electrodynamics experiments in the strong coupling limit. © 2009 Optical Society of America
OCIS codes: 140.3948, 270.0270, 140.7260.

Micropillar optical cavities, typically used in low-threshold vertical-cavity surface-emitting lasers (VCSELs) [1–3], have recently attracted considerable attention as a promising platform for solid-state implementations of cavity quantum electrodynamics (cQED) experiments [4–6]. These applications benefit from a large quality factor (Q) that can be obtained in micropillar cavities, which in turn results in a long photon lifetime $\kappa = \omega/2Q$ (ω is the radial frequency of the cavity mode). For example, high Q micropillar cavities ($Q \sim 165,000$) have been demonstrated recently for large diameter ($d = 4 \mu\text{m}$) pillars, resulting in a relatively large mode volume [$V > 50(\lambda/n)^3$] [7]. However, for applications in cQED it is beneficial to have a small mode volume, since the coupling strength between photon and emitter (g) is proportional to $1/\sqrt{V}$. A small V can be achieved by decreasing the pillar diameter, thus improving the radial confinement of light. Unfortunately, this leads to a significant reduction in the Q factor, and traditional submicrometer diameter micropillars have Q limited to 2000 [8–10].

In this Letter, we for the first time (to our knowledge) theoretically demonstrate submicrometer diameter micropillar cavities with an ultrahigh Q/V that is 3 orders of magnitude larger than previously reported. This is achieved by simultaneously increasing the Q ($Q \sim 3 \times 10^6$) and reducing the mode volume [$V \sim 0.1(\lambda/n)^3$] by using a bandgap tapering method developed recently in one-dimensional (1D) photonic crystal structures [11,12]. While the proposed approach is general and can be applied to a range of material systems and applications, our cavities are designed to operate at 637 nm in wavelength and therefore are suitable for coupling to nitrogen-vacancy (NV) color centers embedded within diamond nanocrystals positioned at the middle of the cavity. NV color centers have recently attracted significant attention as promising quantum emitters [13]. NVs emission is broadband (630–750 nm) with a stable zero-phonon line at 637 nm visible even at room temperature.

Our micropillar is based on two distributed Bragg mirrors (DBRs) that consist of TiO_2 ($n_{\text{TiO}_2} = 2.4$) and

SiO_2 ($n_{\text{SiO}_2} = 1.5$) alternating layers, and a TiO_2 spacer of thickness s sandwiched between them [Fig. 1(a)]. The micropillar cavity Q is inversely proportional to the cavity losses that in turn can be separated into two components: the transmission losses due to the finite length of the DBRs and the scattering losses at the spacer/mirror interfaces. The former can be minimized (for a given number of $\text{TiO}_2/\text{SiO}_2$ pairs) using a “quarter stack” DBR that consists of $\text{TiO}_2/\text{SiO}_2$ layers with thickness $\lambda/4n_{\text{eff}}$, where $\lambda = 637 \text{ nm}$ (n_{eff} is the effective mode index of the segment). This also maximizes light confinement along the pillar axis, resulting in a minimized mode volume. For example, in the case of a micropillar with diameter $d = 340 \text{ nm}$, the thicknesses of TiO_2 and SiO_2 layers in the DBR are 82.6 and 147.4 nm, respectively, resulting in total DBR periodicity of $a = 230 \text{ nm}$. Next, the thickness of the spacer is chosen ($s = 220 \text{ nm}$) to position the cavity resonance at 637 nm, and the quality factor (Q) of such a cavity is obtained using the finite-difference time-domain method (FDTD). We find $Q \sim 100$, which is consistent with previous reports [8]. The low Q is attributed to scattering losses arising from the mode profile mismatch between the localized cavity mode and the

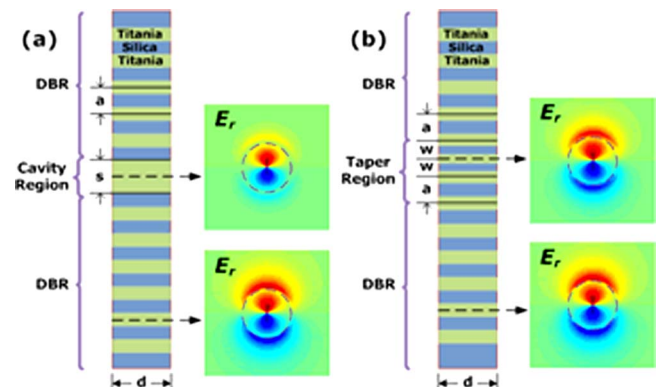


Fig. 1. (Color online) (a) Traditional design of micropillar cavities and (b) modified design, where the center segment is substituted by titania/silica pairs. The lateral mode profile of E_r component for cavity mode and evanescent Bloch mode that exists inside DBRs is shown on the right of the cavity layout. Improved mode-matching can be seen in (b).

evanescent Bloch mode inside the DBRs [14]. Figure 1(a) illustrates the profile mismatch for E_r component. To suppress this mode mismatch and the resulting scattering losses, we use the mode-matching technique previously developed for 1D photonic crystal cavities [11]. We substitute the uniform center segment with a single $\text{TiO}_2/\text{SiO}_2$ pair with the same aspect ratio as in the DBR but a smaller thickness w . When $w=0.67a$, the cavity resonates at $\lambda=637$ nm with $Q=6000$, a 60-fold improvement over the conventional design.

To increase the Q factor further, we incorporate more $\text{TiO}_2/\text{SiO}_2$ segments with varying the thicknesses w_i (i is the segment number). This can also be seen as a “tapered DBR” approach, where each taper section further reduces the mode mismatch to suppress the scattering losses. In Fig. 2(a), we use four tapered segments and 20 DBR pairs at each side. To set the resonating wavelength at 637 nm, the thickness of each taper segment is precisely tuned to $w_1=215.3$, $w_2=202.4$, $w_3=191.0$, and $w_4=180.8$ nm. The resulting mode has a Q factor of 250,000 and a mode volume of $0.07(\lambda/n)^3$, which represents at least 3 orders of magnitude enhancement of Q/V compared to any previous micropillar designs. As shown in Fig. 2(b), this high- Q mode has an antinode at the central TiO_2 segment and therefore is ideally suited for coupling to quantum emitters embedded within this layer. We also find a second-order cavity mode [Fig. 2(c)] at a wavelength of 685 nm with a respectable $Q=110,000$. The Q factor of the fundamental mode can be enhanced by increasing the tapering process. For instance, we obtain $Q=3,000,000$ and $V=0.10(\lambda/n)^3$ with ten taper segments. However, increasing the number of taper segments increases the effective cavity length and pulls higher-order modes from the dielectric band into the bandgap as shown in Figs. 2(d) and 2(e). These higher-order modes can

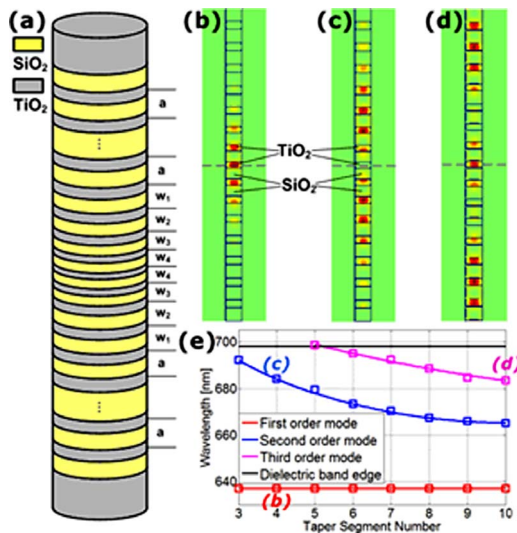


Fig. 2. (Color online) (a) Schematic of a four-taper-segment micropillar cavity. (b) and (c) Electric field density profile of the first- and second-order modes, respectively. (d) Electric field density profile of the third-order mode of the ten-taper-segment micropillar cavity. (e) Mode diagram as a function of taper segment number.

potentially couple to the emitter placed at the center of the cavity, which is not desirable. Therefore from here on we only consider four-taper-segment cavities, which in turn limit our Q to 250,000.

Next, we optimize the diameter of our micropillar cavity to minimize its mode volume. It can be seen in Fig. 3(a) that the smallest mode volume is obtained at $d=340$ nm. For $d < 340$ nm the effective mode index contrast between TiO_2 and SiO_2 is reduced (owing to large evanescent fields) resulting in a narrow photonic bandgap and a larger penetration of the cavity mode into the DBRs (weak axial confinement), thus increasing V . For $d > 340$ nm, however, the mode is almost completely confined within the pillar and the n_{eff} of each segment approaches the refractive index of the material. Therefore, the width of the bandgap remains approximately constant as the pillar diameter increases and the axial confinement remains the same. However, V increases due to the larger mode cross section (radial confinement increases). The trade-off between radial and axial confinement results in an optimized diameter of $d=340$ nm. For the four-taper-segment cavity, we also find the cavity modes with TE_{01} and TM_{01} profiles at wavelengths of 578 and 492 nm, respectively. These modes cannot couple to the NV center placed at the center of the cavity owing to their poor spectral and spatial overlap [Fig. 3(b)] with the NV center. It is also important to note that if the pillar diameter is significantly increased, additional higher-order modes, with the same azimuthal order as HE_{11} (e.g., EH_{11}), are allowed. These modes can couple to the fundamental HE_{11} cavity mode and thus introduce an additional loss mechanism [8] and reduce the Q factor of the fundamental cavity mode.

Finally, we investigate the potential of our microcavity for applications in cQED. Diamond nanocrystals (size < 50 nm) with single NV color centers could be embedded within the central TiO_2 layer in the cavity. It is interesting to note that a refractive index of

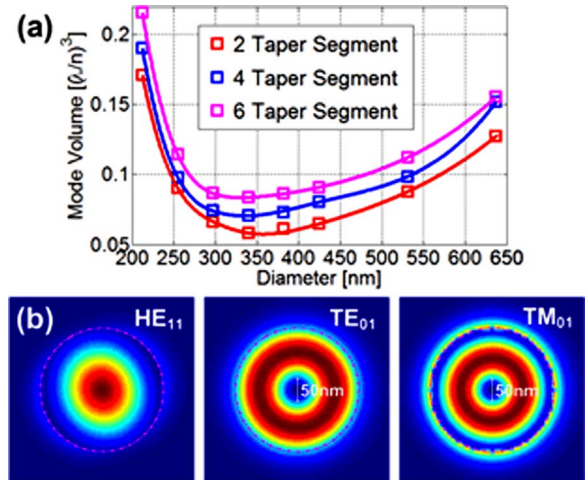


Fig. 3. (Color online) (a) Mode volume as a function of micropillar diameter. Here all the modes are first-order HE_{11} modes resonating at 637 nm. (b) Lateral electric field density profiles of HE_{11} ($\lambda=637$ nm), TE_{01} ($\lambda=578$ nm), and TM_{01} ($\lambda=492$ nm) cavity modes.

TiO₂ is very close to that of a diamond, and therefore the amount of light scattering at the interface between diamond and TiO₂ is negligible. The light-matter interaction process can be characterized by the coupling strength (Rabi frequency) g , the emitter spontaneous emission rate γ , and the photon loss rate κ . The common emission lifetime of a diamond NV center is $\tau \approx 20$ ns, leading to $\gamma = 2\pi/\tau = 2\pi \times 0.05$ GHz. The photon loss rate κ is evaluated via $\kappa = \omega/2Q = 2\pi \times 0.94$ GHz ($Q = 250,000$). Assuming the emitter is positioned at the mode maximum and its dipole moment is parallel to the field vector, the coupling strength can be obtained as $g_0 = \sqrt{3\pi c^3/2\tau\omega^2 n_e n_c^2 V}$, where V is the mode volume of the cavity and n_e and n_c are the refractive indices of the emitter and the cavity, respectively. In a diamond NV center, the zero-phonon line contributes only about 5% of the total emission, the rest being emitted into the phonon sideband. Therefore, only $\approx 5\%$ of the total emission is coupled to the cavity mode, and therefore g must be scaled by a factor of $1/\sqrt{20}$, resulting in $g = g_0/\sqrt{20} = 2\pi \times 7.1$ GHz. By comparing the characteristic frequencies, we conclude that in our system, $g > \kappa$, γ and that the system is well into the strong coupling regime. Furthermore, it is interesting to note that the system is in the strong coupling regime even when $Q > 30,000$, which can be obtained with only ten pairs of DBR mirrors on each side of the tapered section.

In conclusion, we have demonstrated that high- Q factor micropillar cavities can be realized with sub-micrometer diameter pillars. We have engineered the cavities with a record low mode volume and a record high Q and Q/V ratio. We expect, however, that realistic fabricated structures will have a reduced Q owing to fabrication-related imperfections including surface roughness, slanted walls, and material absorption that are not considered in this Letter. One possible approach to overcome some of these problems is based on an oxide-aperture design [15]. We predicted that by embedding a diamond nanocrystal with an NV color center at the middle of the cavity, the strong coupling limit of light-matter interaction can be achieved. Our method can be easily adapted to different material systems and enable realization of an ultrahigh Q/V cavity in an AlAs/GaAs platform suitable for realization of low-threshold VCSELs, for example.

This work was supported in part by National Science Foundation (NSF) grant ECCS-0708905, "Nanoscale Interdisciplinary Research Teams: Photon and Plasmon Engineering in Active Optical Devices based on Synthesized Nanostructures," and Harvard Nanoscale Science and Engineering Centers. The authors acknowledge the assistance provided by Murray W. McCutcheon. Y. Zhang would also like to dedicate this work to Honglie Yin and Erfang Zhang.

References

1. K. Iga, *Jpn. J. Appl. Phys.* **47**, 1 (2008).
2. D. L. Huffaker, Z. Zou, and D. G. Deppe, in *12th Annual Meeting IEEE Lasers and Electro-Optics Society, LEOS '99* (1999), p. 391.
3. S. Reitzenstein, C. Bockler, A. Bazhenov, A. Gorbunov, A. Löffler, M. Kamp, V. D. Kulakovskii, and A. Forchel, *Opt. Express* **16**, 4848 (2008).
4. J. P. Reithmaier, G. Sek, A. Löffler, C. Hofmann, S. Kuhn, S. Reitzenstein, L. V. Keldysh, V. D. Kulakovskii, T. L. Reinecke, and A. Forchel, *Nature* **432**, 197 (2004).
5. D. Press, S. Gotzinger, S. Reitzenstein, C. Hofmann, A. Löffler, M. Kamp, A. Forchel, and Y. Yamamoto, *Phys. Rev. Lett.* **98**, 117402 (2007).
6. J. Vuckovic, M. Pelton, A. Scherer, and Y. Yamamoto, *Phys. Rev. A* **66**, 023808 (2002).
7. S. Reitzenstein, C. Hofmann, A. Gorbunov, M. Gorbunov, M. Straub, S. H. Kwon, C. Schneider, A. Löffler, S. Hoffing, M. Kamp, and A. Forchel, *Appl. Phys. Lett.* **90**, 251109 (2007).
8. P. Lalanne, J. P. Hugonin, and J. M. Gerard, *Appl. Phys. Lett.* **84**, 4726 (2004).
9. G. Lecamp, J. P. Hugonin, P. Lalanne, R. Braive, S. Varoutsis, S. Laurent, A. Lemaitre, I. Sagnes, G. Patriarche, I. Robert-Philip, and I. Abram, *Appl. Phys. Lett.* **90**, 091120 (2007).
10. L. Chen and E. Towe, *Appl. Phys. Lett.* **87**, 103111 (2005).
11. Y. Zhang and M. Loncar, *Opt. Express* **16**, 17400 (2008).
12. M. W. McCutcheon and M. Loncar, *Opt. Express* **16**, 19136 (2008).
13. L. Childress, M. V. G. Dutt, J. M. Taylor, A. S. Zibrov, F. Jelezko, J. Wrachtrup, P. R. Hemmer, and M. D. Lukin, *Science* **314**, 281 (2006).
14. P. Lalanne and J. P. Hugonin, *IEEE J. Quantum Electron.* **39**, 1430 (2003).
15. N. G. Stoltz, M. Rakher, S. Strauf, A. Badolato, D. D. Lofgreen, P. M. Petroff, L. A. Coldren, and D. Bouwmeester, *Appl. Phys. Lett.* **87**, 031105 (2005).